

Sine-Gordon form factors in finite volume

G. Fehér

Budapest University of Technology and Economics
and

G. Takács

HAS Theoretical Physics Research Group
1117 Budapest, Pázmány Péter sétány 1/A, Hungary

21th June 2011

Abstract

We compare form factors in sine-Gordon theory, obtained via the bootstrap, to finite volume matrix elements computed using the truncated conformal space approach. For breather form factors, this is essentially a straightforward application of a previously developed formalism that describes the volume dependence of operator matrix elements up to corrections exponentially decaying with the volume. In the case of solitons, it is necessary to generalize the formalism to include effects of non-diagonal scattering. In some cases it is also necessary to take into account some of the exponential corrections (so-called μ -terms) to get agreement with the numerical data. For almost all matrix elements the comparison is a success, with the puzzling exception of some breather matrix elements that contain disconnected pieces. We also give a short discussion of the implications of the observed behaviour of μ -terms on the determination of operator matrix elements from finite volume data, as occurs e.g. in the context of lattice field theory.

1 Introduction

The matrix elements of local operators (form factors) are central objects in quantum field theory. In two-dimensional integrable quantum field theory the S matrix can be obtained exactly in the framework of factorized scattering developed in [1] (for a later review see [2]). It was shown in [3] that in such theories using the scattering amplitudes as input it is possible to obtain a set of equations satisfied by the form factors. The complete system of form factor equations, which provides the basis for a programmatic approach (the so-called form factor bootstrap) was proposed in [4]. For a detailed and thorough exposition of the subject we refer to [5] on bulk form factors; later this approach was also extended to form factors of boundary operators [6, 7].

Although the connection with the Lagrangian formulation of quantum field theory is rather indirect in the bootstrap approach, it is thought that the general solution of the form factor axioms determines the complete local operator algebra of the theory. This expectation was confirmed in many cases by explicit comparison of the space of solutions

to the spectrum of local operators as described by the ultraviolet limiting conformal field theory [8, 9, 10, 11, 12]; the mathematical foundation is provided by the local commutativity theorem stating that operators specified by solutions of the form factor bootstrap are mutually local [5]. Another important piece of information comes from correlation functions: using form factors, a spectral representation for the correlation functions can be built which provides a large distance expansion [13], while the Lagrangian or perturbed conformal field theory formulation allows one to obtain a short-distance expansion, which can then be compared provided there is an overlap between their regimes of validity [14]. Other evidence for the correspondence between the field theory and the solutions of the form factor bootstrap results from evaluating sum rules like Zamolodchikov’s c -theorem [15, 16, 17, 18] or the Δ -theorem [19], both of which can be used to express conformal data as spectral sums in terms of form factors. Direct comparisons with multi-particle matrix elements are not so readily available, except for perturbative or $1/N$ calculations in some simple cases [3].

Therefore, part of the motivation is to provide non-perturbative evaluation of form factors from the Hamiltonian formulation, which then allows for a direct comparison with solutions of the form factor axioms. Another goal is to have a better understanding of finite size effects in the case of matrix elements of local operators, and to contribute to the investigation of finite volume [20, 21, 22] (and also finite temperature [23]) form factors and correlation functions.

This program has been successfully pursued in the case of diagonal scattering theories (those without particle mass degeneracies), both in the bulk and with boundary [24, 25, 26, 27]. However, an extension to the non-diagonal case is still missing, and the present work is a step in that direction. It is important to realize that non-diagonal theories, whose spectra contain some nontrivial particle multiplets (typically organized into representations of some group symmetry), such as the $O(3)$ nonlinear sigma model are very important for condensed matter applications (e.g. to spin chains; cf. [28]). The finite volume description of form factors can be used to develop a low-temperature and large-distance expansion for finite-temperature correlation functions [25, 29], which could in turn be used to explain experiments such as data from inelastic neutron scattering [30]. Therefore the extension to non-diagonal theories is an interesting direction.

Sine-Gordon model can be considered as the prototype of a non-diagonal scattering theory, and it has the advantage that its finite volume spectra and form factors can be studied numerically using the truncated conformal space approach, originally developed by Yurov and Zamolodchikov for the scaling Lee-Yang model, but later extended to the sine-Gordon theory [31]. Its exact form factors are also known in full generality (at least in principle – see the discussion on multi-soliton form factors later), and so it is a useful playground to test our theoretical ideas on finite volume form factors. This cuts in another way too since our approach also provides a way to test the conjectured exact form factors in much more details than allowed by the usual methods listed above.

The outline of the paper is as follows. We collect the necessary facts about the sine-Gordon form factors in section 2. In Section 3 we turn our attention to the breather form factors, which can be treated by the methods developed for diagonal scattering theories. Section 4 contains our results on soliton form factors, as well as a conjecture how the finite volume form factor formulae derived earlier in [24, 25] can be extended to non-diagonal theories. At present we are only able to perform a partial check of this conjecture due to difficulties in evaluating multi-soliton form factors numerically. Section 5 sums up our conclusions. The paper also contains an appendix devoted to a brief description of the algebraic Bethe Ansatz technique that can be used to obtain the finite volume description of multi-soliton energy levels.

2 Brief review of sine-Gordon form factors

2.1 Action and S matrix

The classical action of the theory is

$$\mathcal{A} = \int d^2x \left(\frac{1}{2} \partial_\mu \Phi \partial^\mu \Phi + \frac{m_0^2}{\beta^2} \cos \beta \Phi \right)$$

The fundamental excitations are a doublet of soliton/antisoliton of mass M . Their exact S matrix can be written as [1]

$$\mathcal{S}_{i_1 i_2}^{j_1 j_2}(\theta, \xi) = S_{i_1 i_2}^{j_1 j_2}(\theta, \xi) S_0(\theta, \xi) \quad (2.1)$$

where

$$\begin{aligned} S_{++}^{++}(\theta, \xi) &= S_{--}^{--}(\theta, \xi) = 1 \\ S_{+-}^{+-}(\theta, \xi) &= S_{-+}^{-+}(\theta, \xi) = S_T(\theta, \xi) \\ S_{+-}^{-+}(\theta, \xi) &= S_{-+}^{+-}(\theta, \xi) = S_R(\theta, \xi) \end{aligned}$$

and

$$\begin{aligned} S_T(\theta, \xi) &= \frac{\sinh\left(\frac{\theta}{\xi}\right)}{\sinh\left(\frac{i\pi-\theta}{\xi}\right)}, \quad S_R(\theta, \xi) = \frac{i \sin\left(\frac{\pi}{\xi}\right)}{\sinh\left(\frac{i\pi-\theta}{\xi}\right)} \\ S_0(\theta, \xi) &= -\exp \left\{ -i \int_0^\infty \frac{dt}{t} \frac{\sinh \frac{\pi(1-\xi)t}{2}}{\sinh \frac{\pi\xi t}{2} \cosh \frac{\pi 2}{2}} \sin \theta t \right\} \\ &= -\left(\prod_{k=1}^n \frac{ik\pi\xi - \theta}{ik\pi\xi + \theta} \right) \exp \left\{ -i \int_0^\infty \frac{dt}{t} \sin \theta t \right. \\ &\quad \left. \times \frac{\left[2 \sinh \frac{\pi(1-\xi)t}{2} e^{-n\pi\xi t} + (e^{-n\pi\xi t} - 1) (e^{\pi(1-\xi)t/2} + e^{-\pi(1+\xi)t/2}) \right]}{2 \sinh \frac{\pi\xi t}{2} \cosh \frac{\pi 2}{2}} \right\} \end{aligned}$$

(the latter representation is valid for any value of $n \in \mathbb{N}$ and makes the integral representation converge faster and further away from the real θ axis).

Besides the solitons, the spectrum of theory contains also breathers B_r , with masses

$$m_r = 2M \sin \frac{r\pi\xi}{2} \quad (2.2)$$

The breather-soliton and breather-breather S -matrices are also known, here we only quote the $B_1 - B_1$ amplitude that is needed in the sequel:

$$\mathcal{S}_{B_1 B_1}(\theta) = \frac{\sinh \theta + i \sin \pi\xi}{\sinh \theta - i \sin \pi\xi} \quad (2.3)$$

Another representation of the theory is as a free massless boson conformal field theory (CFT) perturbed by a relevant operator. The Hamiltonian can be written as

$$H = \int dx \frac{1}{2} : (\partial_t \Phi)^2 + (\partial_x \Phi)^2 : + \mu \int dx : \cos \beta \Phi : \quad (2.4)$$

where the semicolon denotes normal ordering in terms of the modes of the $\mu = 0$ massless field. In this case, due to anomalous dimension of the normal ordered cosine operator, the coupling constant has dimension

$$\mu \sim [\text{mass}]^{2-\beta^2/4\pi}$$

2.2 Breather form factors

We consider only exponentials of the bosonic field Φ . To obtain matrix elements containing the first breather, one can analytically continue the form factors of sinh-Gordon theory obtained in [8] to imaginary values of the couplings. The result is

$$\begin{aligned} F_{\underbrace{11\dots 1}_n}^a(\theta_1, \dots, \theta_n) &= \langle 0 | e^{ia\beta\Phi(0)} | B_1(\theta_1) \dots B_1(\theta_n) \rangle \\ &= \mathcal{G}_a(\beta) [a]_\xi (i\bar{\lambda}(\xi))^n \prod_{i<j} \frac{f_\xi(\theta_j - \theta_i)}{e^{\theta_i} + e^{\theta_j}} Q_a^{(n)}(e^{\theta_1}, \dots, e^{\theta_n}) \end{aligned} \quad (2.5)$$

where

$$\begin{aligned} Q_a^{(n)}(x_1, \dots, x_n) &= \det[a + i - j]_\xi \sigma_{2i-j}^{(n)}(x_1, \dots, x_n)_{i,j=1,\dots,n-1} \text{ if } n \geq 2 \\ Q_a^{(1)} &= 1, \quad [a]_\xi = \frac{\sin \pi \xi a}{\sin \pi \xi} \\ \bar{\lambda}(\xi) &= 2 \cos \frac{\pi \xi}{2} \sqrt{2 \sin \frac{\pi \xi}{2}} \exp \left(- \int_0^{\pi \xi} \frac{dt}{2\pi} \frac{t}{\sin t} \right) \end{aligned}$$

and

$$\begin{aligned} f_\xi(\theta) &= v(i\pi + \theta, -1)v(i\pi + \theta, -\xi)v(i\pi + \theta, 1 + \xi) \\ &\quad v(-i\pi - \theta, -1)v(-i\pi - \theta, -\xi)v(-i\pi - \theta, 1 + \xi) \\ v(\theta, \zeta) &= \prod_{k=1}^N \left(\frac{\theta + i\pi(2k + \zeta)}{\theta + i\pi(2k - \zeta)} \right)^k \exp \left\{ \int_0^\infty \frac{dt}{t} \left(-\frac{\zeta}{4 \sinh \frac{t}{2}} - \frac{i\zeta\theta}{2\pi \cosh \frac{t}{2}} \right. \right. \\ &\quad \left. \left. + (N + 1 - Ne^{-2t}) e^{-2Nt + \frac{i\theta}{\pi}} \frac{\sinh \zeta t}{2 \sinh^2 t} \right) \right\} \end{aligned} \quad (2.6)$$

gives the minimal $B_1 B_1$ form factor¹, while $\sigma_k^{(n)}$ denotes the elementary symmetric polynomial of n variables and order k defined by

$$\prod_{i=1}^n (x + x_i) = \sum_{k=0}^n x^{n-k} \sigma_k^{(n)}(x_1, \dots, x_n)$$

Furthermore

$$\begin{aligned} \mathcal{G}_a(\beta) = \langle e^{ia\beta\Phi} \rangle &= \left[\frac{M \sqrt{\pi} \Gamma \left(\frac{4\pi}{8\pi - \beta^2} \right)}{2\Gamma \left(\frac{\beta^2/2}{8\pi - \beta^2} \right)} \right]^{\frac{a^2 \beta^2}{4\pi}} \exp \left\{ \int_0^\infty \frac{dt}{t} \left[-\frac{a^2 \beta^2}{4\pi} e^{-2t} \right. \right. \\ &\quad \left. \left. + \frac{\sinh^2 \left(\frac{a}{4\pi} t \right)}{2 \sinh \left(\frac{\beta^2}{8\pi} t \right) \cosh \left(\left(1 - \frac{\beta^2}{8\pi} \right) t \right) \sinh t} \right] \right\} \end{aligned} \quad (2.7)$$

is the exact vacuum expectation value of the exponential field [32], with M denoting the soliton mass related to the coupling μ defined in via [33]

$$\mu = \frac{2\Gamma(\Delta)}{\pi\Gamma(1-\Delta)} \left(\frac{\sqrt{\pi}\Gamma \left(\frac{1}{2-2\Delta} \right) M}{2\Gamma \left(\frac{\Delta}{2-2\Delta} \right)} \right)^{2-2\Delta}, \quad \Delta = \frac{\beta^2}{8\pi} \quad (2.8)$$

Formula (2.5) also coincides with the result given in [34]. Form factors of higher breathers can be constructed by considering them as bound states of B_1 particles. Detailed formulae can be found in Appendix A of [35].

¹The formula for the function v is in fact independent of N ; choosing N large extends the width of the strip where the integral converges and also speeds up convergence.

2.3 Soliton form factors

At present, there are three independent constructions of solitonic form factors available: the earliest one by Smirnov (reviewed in [36]), the free field representation by Lukyanov [37, 34] and the work by Babujian et al. [38, 39]. Here we use formulae from Lukyanov's work [34]. The simplest form factor for an exponential operator is with a soliton-antisoliton state and it takes the form

$$\begin{aligned} \langle 0 | e^{i\beta\Phi(0)} | S_{\pm}(\theta_2) S_{\mp}(\theta_1) \rangle &= F_{\mp\pm}^{\beta}(\theta_1 - \theta_2) \\ F_{\mp\pm}^{\beta}(\theta) &= \mathcal{G}_1(\beta) G(\theta) \cot\left(\frac{\pi\xi}{2}\right) \frac{4i \cosh\left(\frac{\theta}{2}\right) e^{\mp\frac{\theta+i\pi}{2\xi}}}{\xi \sinh\left(\frac{\theta+i\pi}{\xi}\right)} \end{aligned} \quad (2.9)$$

where S_+ and S_- denote the soliton and antisoliton, respectively. The function G is given by the integral representation

$$\begin{aligned} G(\theta) &= i \sinh\left(\frac{\theta}{2}\right) \exp\left\{ \int_0^\infty \frac{dt}{t} \sinh^2\left(\left(1 - \frac{i\theta}{\pi}\right)t\right) \frac{\sinh(t(\xi - 1))}{\sinh(2t) \cosh(t) \sinh(t\xi)} \right\} \\ &= i \sinh\left(\frac{\theta}{2}\right) \prod_{k=1}^N g(\theta, \xi, k)^k \exp\left\{ \int_0^\infty \frac{dt}{t} e^{-4Nt} (1 + N - N e^{-4t}) \right. \\ &\quad \times \left. \sinh^2\left(\left(1 - \frac{i\theta}{\pi}\right)t\right) \frac{\sinh(t(\xi - 1))}{\sinh(2t) \cosh(t) \sinh(t\xi)} \right\} \\ g(\theta, \xi, k) &= \frac{\Gamma\left(\frac{(2k+1+\xi)\pi-i\theta}{\pi\xi}\right) \Gamma\left(\frac{2k+1}{\xi}\right)^2 \Gamma\left(\frac{(2k+1)\pi-i\theta}{\pi\xi}\right)}{\Gamma\left(\frac{2k+\xi}{\xi}\right)^2 \Gamma\left(\frac{(2k+\xi)\pi-i\theta}{\pi\xi}\right) \Gamma\left(\frac{(2k-2+\xi)\pi+i\theta}{\pi\xi}\right)} \\ &\quad \times \frac{\Gamma\left(\frac{(2k-1)\pi+i\theta}{\pi\xi}\right) \Gamma\left(\frac{2k-1+\xi}{\xi}\right)^2 \Gamma\left(\frac{(2k-1+\xi)\pi+i\theta}{\pi\xi}\right)}{\Gamma\left(\frac{2k}{\xi}\right)^2 \Gamma\left(\frac{(2k+2)\pi-i\theta}{\pi\xi}\right) \Gamma\left(\frac{2k\pi+i\theta}{\pi\xi}\right)} \end{aligned}$$

where, again, the second formula is eventually independent of the natural number N ; it provides a representation which converges faster numerically and is valid further away from the real θ axis with increasing N .

Higher form factors in all the available constructions are given in some quite complicated integral representation which we do not write down here. We have been unable to find a numerical evaluation of these analytic formulae at present, which precludes their use in a comparison with TCSA data.

3 Breather form factors in finite volume

3.1 A review of the theoretical predictions

As breathers are singlet and so scatter diagonally, the formulae presented in the papers [24, 25] are directly applicable. The first ingredient is to describe the multi-breather energy levels corresponding to the states

$$|B_{r_1}(\theta_1) \dots B_{r_N}(\theta_N)\rangle$$

whose finite volume counter part we are going to label

$$|\{I_1, \dots, I_N\}\rangle_{r_1 \dots r_N, L}$$

where the I_k are the momentum quantum numbers. In a finite volume L , momentum quantization is governed (up to corrections decreasing exponentially with L) by the Bethe-Yang equations:

$$Q_k(\theta_1, \dots, \theta_n) = m_{r_k} L \sinh \theta_k + \sum_{j \neq k} \delta_{r_j r_k} (\theta_k - \theta_j) = 2\pi I_k \quad I_k \in \mathbb{Z} \quad (3.1)$$

where the phase-shift is defined as

$$S_{B_r B_s}(\theta) = e^{i\delta_{sr}(\theta)}$$

In practical calculations, because breathers of the same species satisfy an effective exclusion rule due to

$$S_{B_r B_r}(0) = -1$$

it is best to redefine phase-shifts corresponding to them by extracting a $-$ sign:

$$S_{B_r B_r}(\theta) = -e^{i\delta_{rr}(\theta)}$$

so that $\delta_{sr}(0) = 0$ can be taken for all s, r and all the phase-shifts can be defined as continuous functions over the whole real θ axis. This entails shifting appropriate quantum numbers I_k to half-integer values. Given a solution $\tilde{\theta}_1, \dots, \tilde{\theta}_N$ to the quantization relations (3.1) the energy and the momentum of the state can be written as

$$\begin{aligned} E &= \sum_{k=1}^N m_{r_k} \cosh \tilde{\theta}_k \\ P &= \sum_{k=1}^N m_{r_k} \sinh \tilde{\theta}_k = \frac{2\pi}{L} \sum_k I_k \end{aligned}$$

(using that $-$ with our choice of the phase-shift functions $-$ unitarity entails $\delta_{sr}(\theta) + \delta_{rs}(-\theta) = 0$). The rapidity-space density of n -particle states can be calculated as

$$\rho_{r_1 \dots r_n}(\theta_1, \dots, \theta_n) = \det \mathcal{J}^{(n)} \quad , \quad \mathcal{J}_{kl}^{(n)} = \frac{\partial Q_k(\theta_1, \dots, \theta_n)}{\partial \theta_l} \quad , \quad k, l = 1, \dots, n \quad (3.2)$$

The matrix elements of local operators between finite volume multi-particle states can be written as [24]

$$\begin{aligned} &|_{s_1 \dots s_M} \langle \{I'_1, \dots, I'_M\} | \mathcal{O}(0, 0) | \{I_1, \dots, I_N\} \rangle_{r_1 \dots r_N, L} = \\ &\left| \frac{F_{s_M \dots s_1 r_1 \dots r_N}^{\mathcal{O}}(\tilde{\theta}'_M + i\pi, \dots, \tilde{\theta}'_1 + i\pi, \tilde{\theta}_1, \dots, \tilde{\theta}_N)}{\sqrt{\rho_{r_1 \dots r_N}(\tilde{\theta}_1, \dots, \tilde{\theta}_N) \rho_{s_1 \dots s_M}(\tilde{\theta}'_1, \dots, \tilde{\theta}'_M)}} \right| + O(e^{-\mu' L}) \end{aligned} \quad (3.3)$$

(note that we cannot specify the phase of the matrix elements as it depends on phase conventions which can be different in finite and infinite volume) which is valid provided there are no disconnected terms. Such terms appear when there are two breathers of the same species in the two states whose rapidities coincide. Apart from some very special cases, this happens only when the two states are identical, which is called the diagonal matrix element. The necessary formulae are written down in [25]; instead of quoting here the rather lengthy general expression, we present the two particular cases we need:

$$\begin{aligned} {}_1 \langle \{I\} | \mathcal{O}(0, 0) | \{I\} \rangle_{1, L} &= \frac{F_{11}^{\mathcal{O}}(i\pi, 0)}{m_1 L \cosh \tilde{\theta}} + \langle \mathcal{O} \rangle + O(e^{-\mu' L}) \\ {}_{11} \langle \{I_1, I_2\} | \mathcal{O}(0, 0) | \{I_1, I_2\} \rangle_{11, L} &= \frac{\mathcal{F}_{11}^{\mathcal{O}}(\tilde{\theta}_1, \tilde{\theta}_2) + m_1 L (\cosh \tilde{\theta}_1 + \cosh \tilde{\theta}_2) F_{11}^{\mathcal{O}}(i\pi, 0)}{\rho_{11}(\tilde{\theta}_1, \tilde{\theta}_2)} \\ &\quad + \langle \mathcal{O} \rangle + O(e^{-\mu' L}) \end{aligned} \quad (3.4)$$

where

$$\langle \mathcal{O} \rangle$$

is the vacuum expectation value of the local operator \mathcal{O} and

$$\mathcal{F}_{11}^{\mathcal{O}}(\theta_1, \theta_2) = \lim_{\epsilon \rightarrow 0} F_{1111}^{\mathcal{O}}(\theta_2 + i\pi + \epsilon, \theta_1 + i\pi + \epsilon, \theta_1, \theta_2)$$

is the so-called symmetric evaluation of the four-particle form factor. Note that in the diagonal case there is no possible phase difference between the finite-volume matrix elements and the infinite volume form factors, as any phase redefinition of the state drops out from the matrix element.

The above predictions for finite volume energy levels and matrix elements are expected to be exact to all (finite) orders in $1/L$ [24, 25] (note that the exponential corrections are non-analytic in this variable).

3.2 Numerical results

To evaluate the form factors numerically, we use the truncated conformal space approach (TCSA) pioneered by Yurov and Zamolodchikov [40]. The extension to the sine-Gordon model was developed in [31] and has found numerous applications since then. The Hilbert space can be split by the eigenvalues of the topological charge \mathcal{Q} (or winding number) and the spatial momentum P , where the eigenvalues of the latter are of the form

$$\frac{2\pi s}{L}$$

s is called the ‘conformal spin’.

In sectors with vanishing topological charge, we can make use of the symmetry of the Hamiltonian under

$$\mathcal{C} : \quad \Phi(x, t) \rightarrow -\Phi(x, t)$$

which is equivalent to conjugation of the solitonic charge. The truncated space can be split into \mathcal{C} -even and \mathcal{C} -odd subspaces that have roughly equal dimensions, which speeds up the diagonalization of the Hamiltonian by roughly a factor of eight (the required machine time scales approximately with the third power of matrix size). We remark that there is another discrete symmetry

$$\mathcal{P} : \quad \Phi(x, t) \rightarrow -\Phi(-x, t)$$

corresponding to spatial parity, which is a symmetry in $s = 0$ sectors. However, we use the $s \neq 0$ states extensively in our calculations.

For the calculations, we choose the operator

$$\mathcal{O} =: e^{i\beta\Phi} :$$

which is essentially one half of the interaction term in the Hamiltonian in (2.4). The semicolons denote normal ordering with respect to the $\lambda = 0$ free massless boson modes. This operator has conformal dimension

$$\Delta_{\mathcal{O}} = \bar{\Delta}_{\mathcal{O}} = \frac{\beta^2}{8\pi}$$

Using relation (2.8) we can express all energy levels and matrix elements in units of (appropriate powers of) the soliton mass M , and we also introduce the dimensionless volume variable $l = ML$. The general procedure is the same as in [24, 25]: the particle content of energy levels can be identified by matching the numerical TCSA spectrum against the

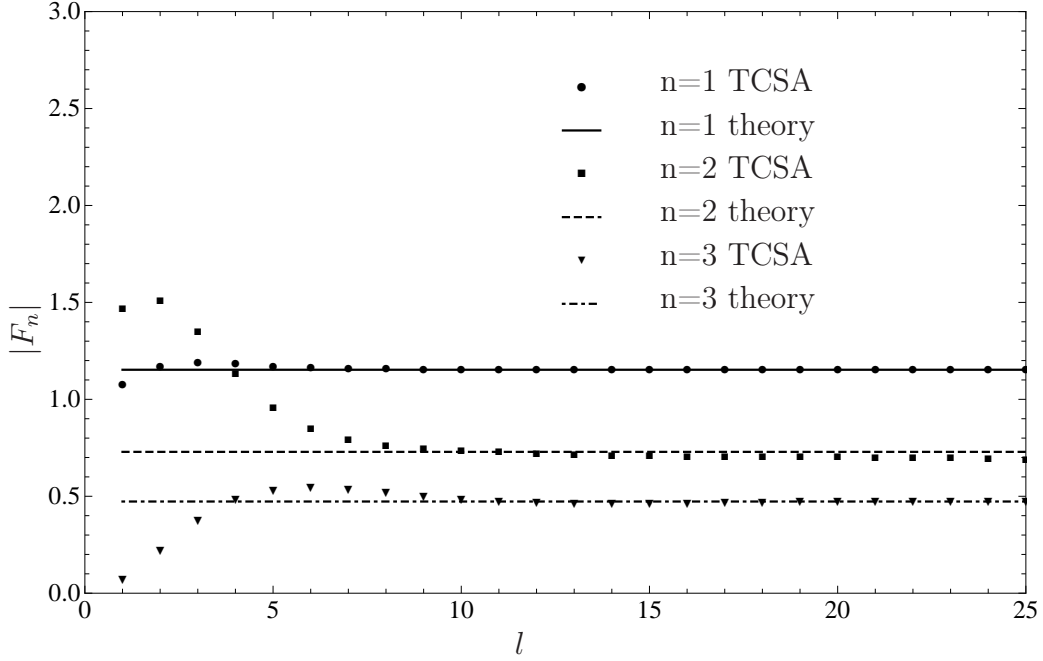


Figure 3.1: One-particle form factors at $\xi = 50/239$

predictions of the Bethe-Yang equations (3.1). After identification, one can compare the appropriate matrix elements to the theoretical values given by (3.3) and (3.4).

Due to level crossings, at certain values of the volume L there can be more than one TCSA candidate levels for a given Bethe-Yang solution; identification can be completed by selecting the candidate on the basis of one of the form factor measurements, which still leaves other matrix elements involving the state as cross-checks. Level crossings also present a problem in numerical stability, since in their vicinity the state of interest is nearly degenerate to another one. Since the truncation effect can be considered as an additional perturbing operator, the level crossings are eventually lifted. However, such a near-degeneracy greatly magnifies truncation effects on the eigenvectors and therefore the matrix elements [27]. This is the reason behind the fact that in some of the figures there are some individual numerical points that are clearly scattered away from their expected place.

The simplest matrix element to test is the theoretical prediction (2.7) for the exact vacuum expectation value, and we did check it against the numerical results. However, it has already been subjected to extensive verification against TCSA in [41], therefore we do not dwell on this issue here.

One-particle form factors can be tested using a reorganized form of the relation (3.3):

$$|F_n^{\mathcal{O}}| = |\langle 0 | e^{i\beta\Phi(0)} | B_n(0) \rangle| = \left| \sqrt{m_n L} \langle 0 | e^{i\beta\Phi(0)} | \{0\} \rangle_{n,L} \right| + O(e^{-\mu' L})$$

(the form factors themselves are independent of the rapidity of the particle due to Lorentz invariance). For the lowest three breathers the agreement between numerics and theory is illustrated in figure 3.1.

The next interesting matrix element is the two-particle one, for which we can use the relation

$$|F_{11}^{\mathcal{O}}(\tilde{\theta}_1, \tilde{\theta}_2)| = \left| \langle 0 | e^{i\beta\Phi(0)} | B_1(\tilde{\theta}_1) B_1(\tilde{\theta}_2) \rangle \right| = \left| \sqrt{\rho_{11}(\tilde{\theta}_1, \tilde{\theta}_2)} \langle 0 | e^{i\beta\Phi(0)} | \{I_1, I_2\} \rangle_{11,L} \right| + O(e^{-\mu' L})$$

which is tested in figure 3.2. This provides a test of the two-particle form factor for real rapidity differences. However, the two-particle form factor function also appears in the

(off-diagonal and diagonal) B_1 - B_1 matrix elements

$$\begin{aligned} \left| {}_1 \langle \{I'\} | e^{i\beta\Phi(0)} | \{I\} \rangle_{1,L} \right| &= \frac{|F_{11}^{\mathcal{O}}(i\pi + \tilde{\theta}', \tilde{\theta})|}{m_1 L \sqrt{\cosh \tilde{\theta}' \cosh \tilde{\theta}}} + O(e^{-\mu' L}) \\ {}_1 \langle \{I\} | e^{i\beta\Phi(0)} | \{I\} \rangle_{1,L} &= \frac{F_{11}^{\mathcal{O}}(i\pi, 0)}{m_1 L \cosh \tilde{\theta}} + \mathcal{G}_1(\beta) + O(e^{-\mu' L}) \end{aligned}$$

which makes it possible to test the form factor for rapidity differences with imaginary part π as shown in figures 3.3 and 3.4. We remark that in plots against rapidity the small-rapidity deviations are due to truncation errors, while the ones for large rapidity result from the neglected exponential corrections.

We can also test the three and four particle form-factors using $B_1 - B_1 B_1$ and off-diagonal $B_1 B_1 - B_1 B_1$ matrix elements, as shown in figures 3.5 and 3.6. Diagonal $B_1 B_1 - B_1 B_1$ matrix elements reveal some complications, and are treated in subsection 3.4.

All of these tests show excellent agreement between numerics and theory, which make us confident both in the finite volume form factor formalism and the correctness of the exact form factors (2.5) predicted by the bootstrap.

3.3 B_2 matrix elements and μ -terms

We can also use the identified B_2 state to compute matrix elements involving it. However, in some cases simply using (3.3) gives a rather poor match. It turns out that accounting for some of the hitherto neglected exponential corrections can improve this; the leading corrections come from so-called μ -terms which were constructed in [42] building upon the ideas in Lüscher's seminal paper [43]. We remark that the method outlined below eventually does more; it entails a resummation of these correction beyond the mere construction of the leading exponential correction.

Using the ideas in [42], we can model a finite volume B_2 state as a pair of B_1 particles with complex conjugate rapidities by solving the $B_1 B_1$ Bethe-Yang equations (here written in exponential form):

$$e^{im_1 L \sinh(\theta \pm iu)} S_{B_1 B_1}(\pm 2iu) = 1 \quad (3.5)$$

The solution for u has the large volume behaviour

$$u \sim \frac{\pi\xi}{2} + C e^{-\mu L \cosh \theta} \quad (3.6)$$

with

$$\mu = \sqrt{m_1^2 - \frac{m_2^2}{4}} = m_1 \sin \frac{\pi\xi}{2}$$

and C some numerical constant. Therefore, for $L \rightarrow \infty$ one obtains the usual bootstrap identification

$$B_2(\theta) \simeq B_1(\theta + i\pi\xi/2) B_1(\theta - i\pi\xi/2)$$

and the momentum and energy of the state tends to

$$\begin{aligned} m_1 \sinh(\theta + iu) + m_1 \sinh(\theta - iu) &= 2m_1 \cos u \sinh \theta \xrightarrow{L \rightarrow \infty} m_2 \sinh \theta \\ m_1 \cosh(\theta + iu) + m_1 \cosh(\theta - iu) &= 2m_1 \cos u \cosh \theta \xrightarrow{L \rightarrow \infty} m_2 \cosh \theta \end{aligned}$$

where

$$m_2 = 2m_1 \cos \frac{\pi\xi}{2}$$

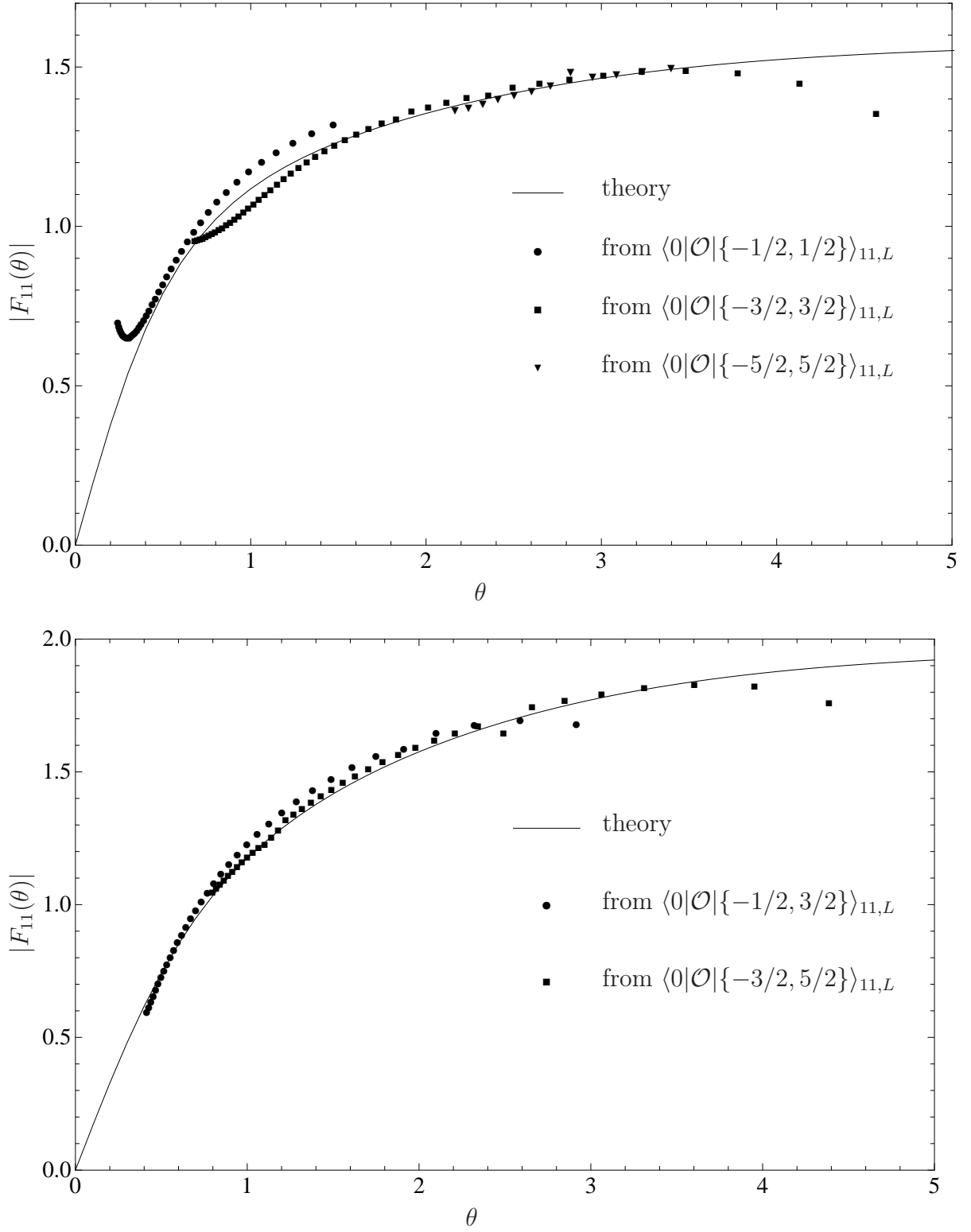


Figure 3.2: $B_1 B_1$ two-particle form factors. The first plot shows spin-0 data with $\xi = 50/239$, while the second one shows spin-1 data with $\xi = 2/7$.

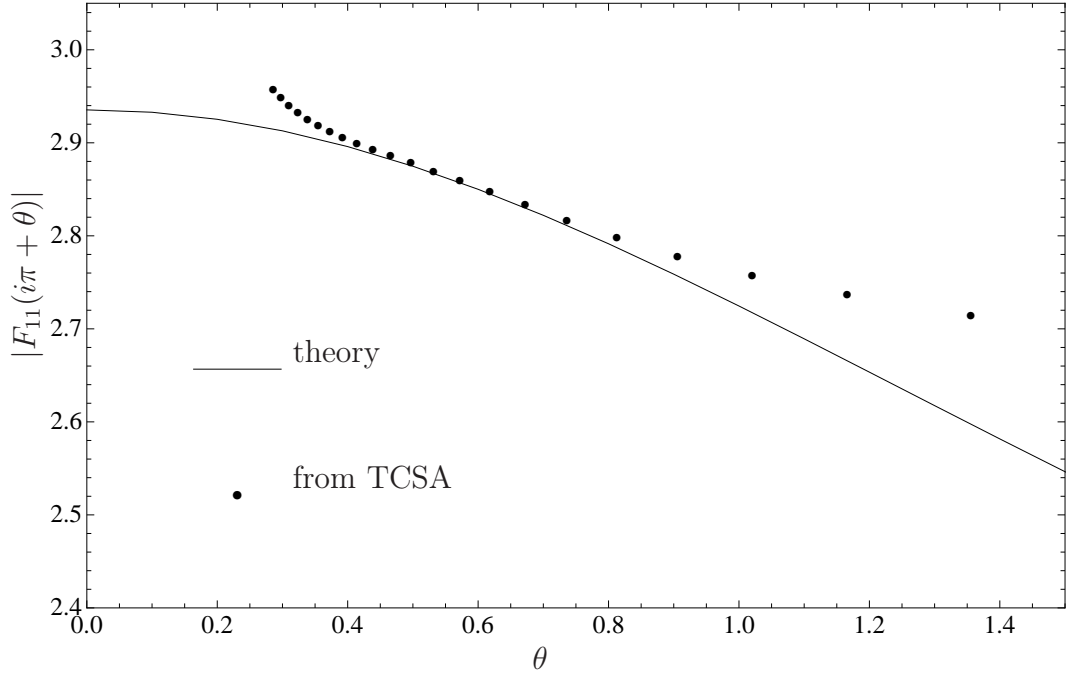


Figure 3.3: Crossed $B_1 B_1$ two-particle form factor. The TCSA measurements are taken from the matrix element ${}_1\langle\{1\}|\mathcal{O}|\{0\}\rangle_1$ at $\xi = 2/7$.

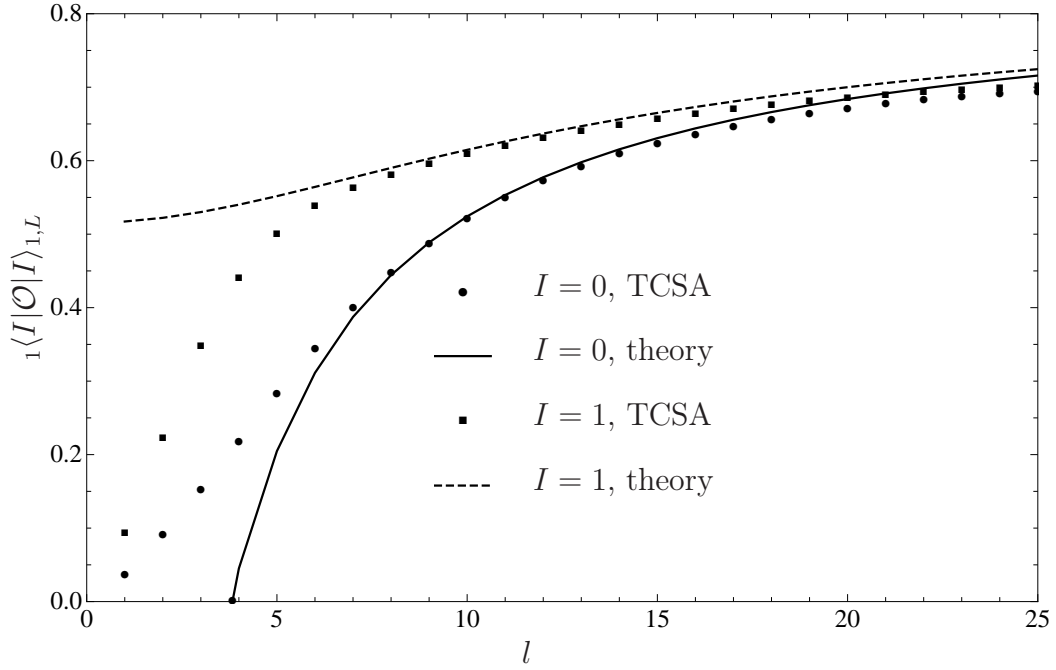


Figure 3.4: Diagonal B_1 - B_1 matrix elements at $\xi = 50/239$.

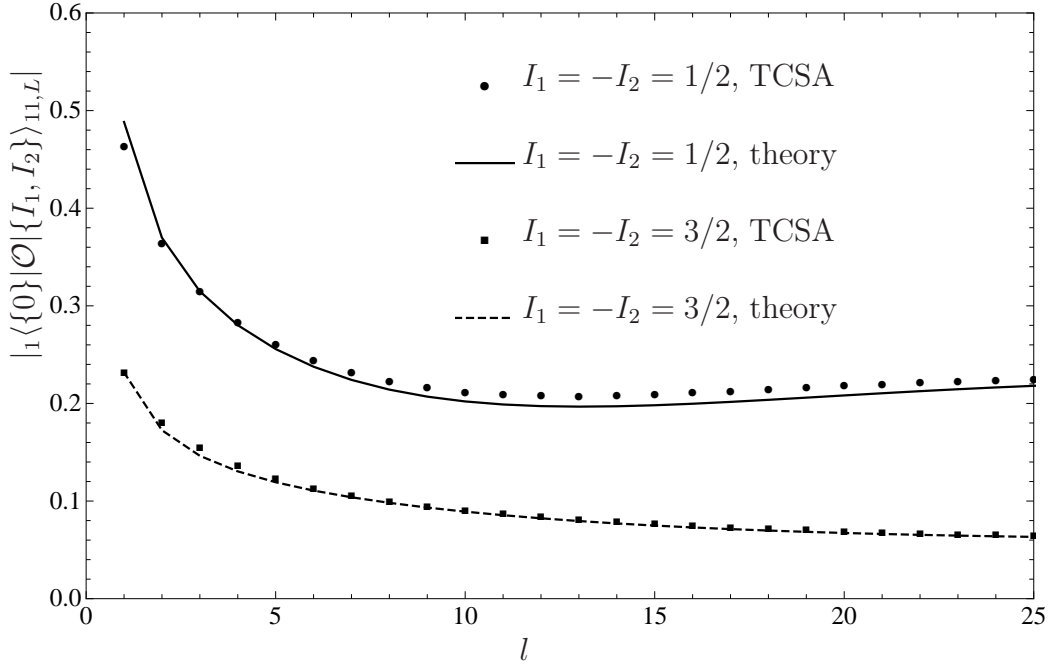


Figure 3.5: B_1 - $B_1 B_1$ matrix elements at $\xi = 50/239$.

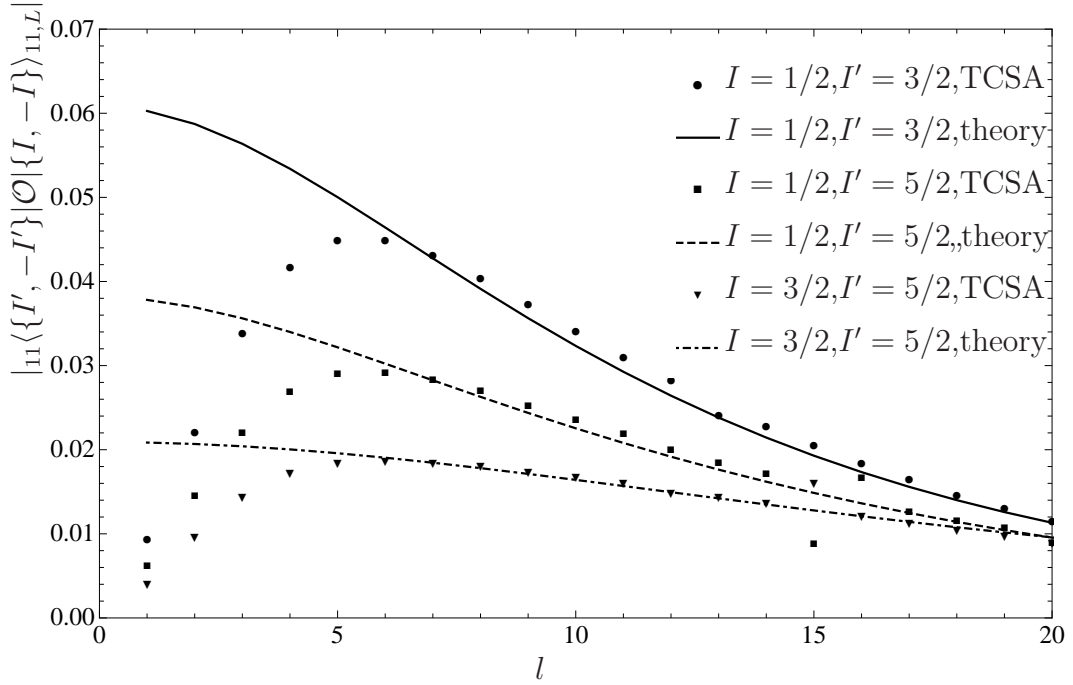


Figure 3.6: Off-diagonal $B_1 B_1$ - $B_1 B_1$ matrix elements at $\xi = 50/239$. The individual deviations are caused by the proximity of level crossings.

is the mass of B_2 in terms of that of B_1 , consistent with (2.2).

In order to do this, however, formula (3.3) must be continued to complex rapidities, which requires matching the phases of the matrix elements on the two sides. This is not difficult to do by observing that the TCSA matrix elements are all real², while the phase of the minimal form factor function $f_\xi(\theta)$ (2.6) is just half the phase of the two-particle S -matrix $S_{B_1 B_1}(\theta)$. Using the results of [42] one obtains

$$\langle 0 | \mathcal{O}(0, 0) | \{I\} \rangle_{2,L} = \pm \frac{\sqrt{S_{B_1 B_1}(-2i\tilde{u})} F_{11}^{\mathcal{O}}(\tilde{\theta} + i\tilde{u}, \tilde{\theta} - i\tilde{u})}{\sqrt{\rho_{11}(\tilde{\theta} + i\tilde{u}, \tilde{\theta} - i\tilde{u})}} + \dots$$

where $\tilde{\theta}, \tilde{u}$ is the solution of (3.5) with the correct momentum, ie.

$$m_1 L \sinh(\tilde{\theta} + i\tilde{u}) + m_1 L \sinh(\tilde{\theta} - i\tilde{u}) = 2\pi I$$

and the dots denote further (and generally much smaller) exponential corrections; the \pm sign accounts for the remaining phase ambiguity from the square root. One can similarly evaluate $B_1 - B_2$ matrix elements using

$$|{}_1\langle \{I'\} | \mathcal{O}(0, 0) | \{I\} \rangle_{2,L}| = \frac{\left| \sqrt{S_{B_1 B_1}(-2i\tilde{u})} F_{111}^{\mathcal{O}}(i\pi + \tilde{\theta}', \tilde{\theta} + i\tilde{u}, \tilde{\theta} - i\tilde{u}) \right|}{\sqrt{m_1 L \cosh \tilde{\theta}' \rho_{11}(\tilde{\theta} + i\tilde{u}, \tilde{\theta} - i\tilde{u})}} + \dots$$

where the absolute values are necessary because we have not compensated for the phase difference due to the presence of the additional B_1 . We observed substantial improvement over the naive matrix elements (3.3) that neglect the μ -term contributions; some of our data are demonstrated in figure 3.7. The effect is very dramatic for the $B_1 - B_2$ case, the naive prediction drastically disagrees with the numerical results, while the inclusion of the μ -terms leads to excellent agreement. This is in fact a bit unexpected, as the value for the exponent for $\xi = 2/7$ is

$$\mu L = \sqrt{m_1^2 - \frac{m_2^2}{4}} L \approx 0.37651 l \quad , \quad l = ML$$

whose coefficient is not particularly small. In the original example in [42] one of the particles was loosely bound, resulting in a very small value for μ , which in turn led to large finite size corrections from the particle splitting up in finite volume. This is not case for B_2 considered as a bound state of two B_1 s at the particular value of the coupling ξ in question. However, the full behaviour is determined not only by the exponent, but also by the detailed behaviour of the S -matrix amplitude and the form factor near the pole; it is the latter that enhances the correction in the $B_1 - B_2$ case. We return to this observation and its implications in the conclusion.

3.4 Diagonal $B_1 B_1 - B_1 B_1$ matrix elements

For the diagonal matrix element we observe significant difference between the numerical results and the theoretical predictions as shown in figure 3.8. It is apparent from the data that agreement is better for lower values of ξ . For large volumes, this is easily explained by the better convergence of TCSA since the dominant source of errors in the large volume

²This is the case because the TCSA representation of the Hamiltonian turns out to be a real and symmetric matrix, due to the fact that the matrix elements of operators $e^{ia\beta\Phi}$ are all real. As a results, all eigenvectors are also real and therefore all the matrix elements computed from TCSA are real as well.

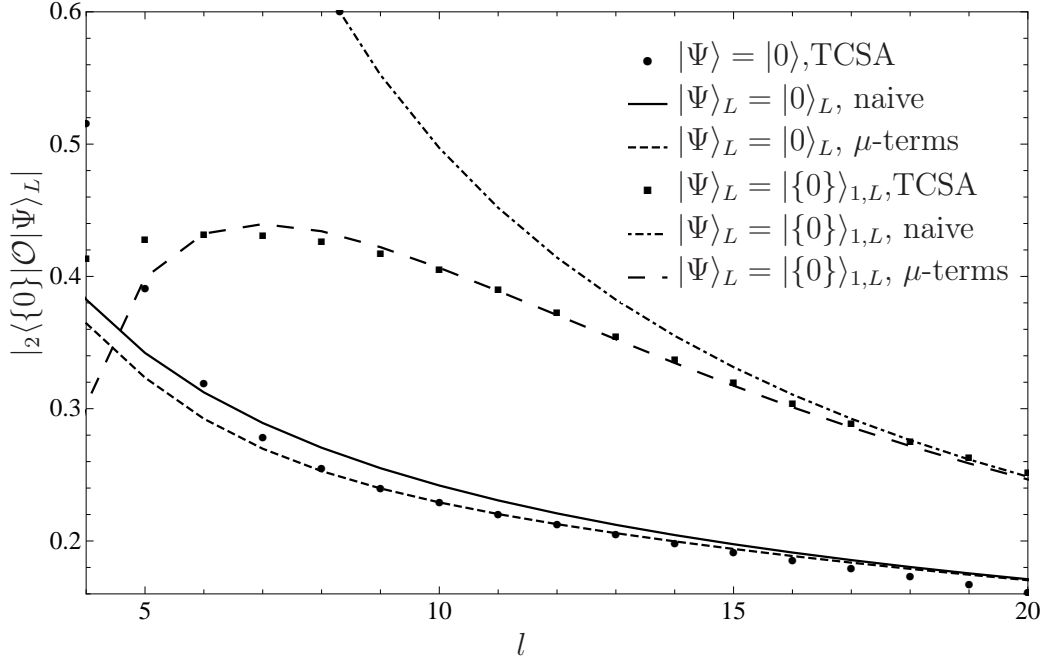


Figure 3.7: Naive predictions for matrix elements involving B_2 , together with ones including μ -term corrections compared to numerical data for the B_2 -vacuum and $B_2 - B_1$ matrix elements at $\xi = 2/7$.

data is the Hilbert space truncation, and improvement of truncation errors with decreasing ξ was observed in all the data we analyzed.

However, this cannot be the origin the deviation in the medium range of volume ($5 \lesssim l \lesssim 15$). This deviation also decreases for smaller ξ , and is likely to have its origin in a μ -term correction. Evaluating such a μ -term requires modeling B_1 as a soliton-antisoliton bound state, which we are not able to do at present as it necessitates numerically handling eight-particle solitonic form factors. As for the variation of the μ -term with ξ , analogous behaviour was observed for the B_2 case, where we also have analytic confirmation of the numerical results.

3.5 Higher breathers

We also tested numerous other form factors including higher breathers (among them $B_2 - B_1 B_1$, $B_2 - B_2$, $B_1 - B_3$, $B_2 - B_3$ and $B_3 - B_3$ matrix elements), and in all cases found good agreement between theoretical predictions and TCSA data. These tests cover all multi- B_1 form factors (2.5) up to 6 particles (taking into account that B_n is obtained as a fusion of n first breathers, as described in Appendix A of [35]).

4 Soliton form factors in finite volume

4.1 Finite volume form factors in non-diagonal theories

We can follow the lines of the reasoning in [24] that lead to the formula for the finite volume form factors. We recall the main outlines of the arguments, making modifications where

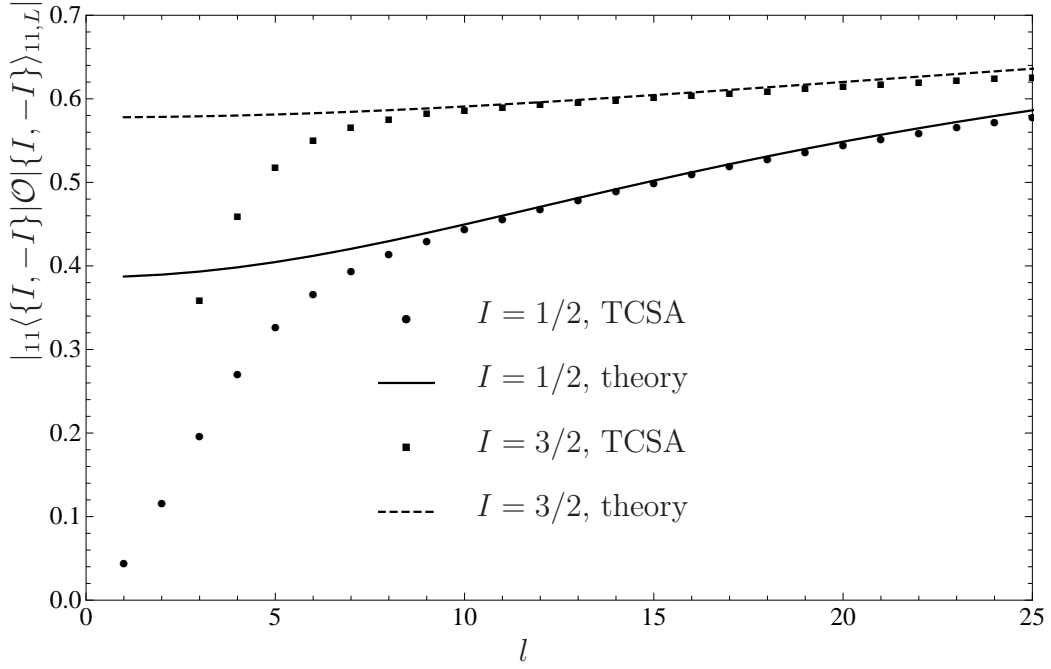
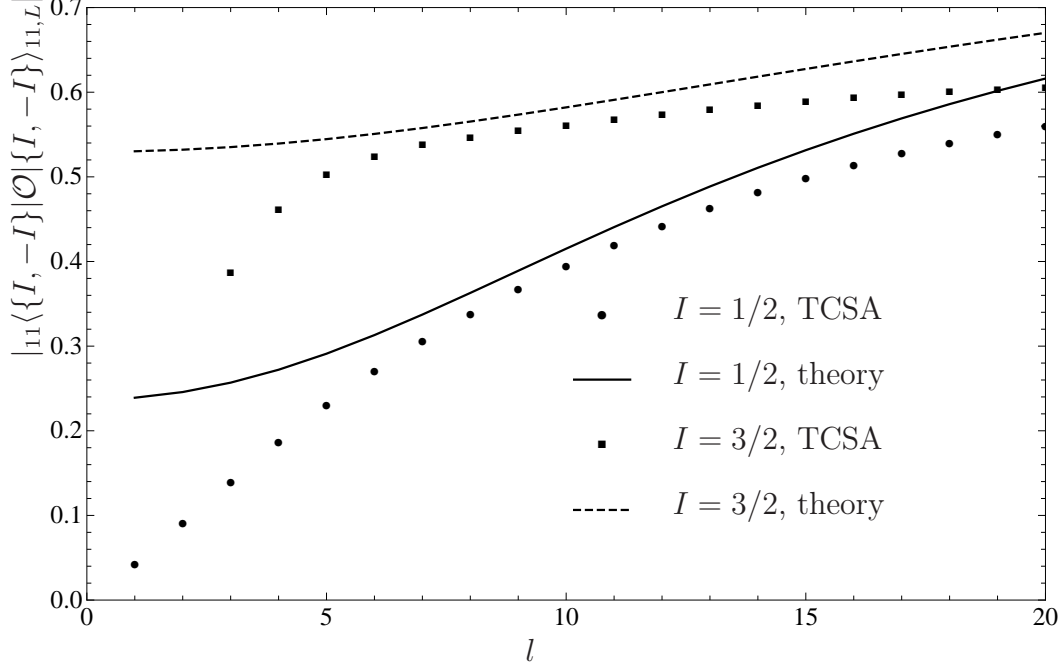


Figure 3.8: Diagonal $B_1 B_1 - B_1 B_1$ matrix elements for $\xi = 2/7$ and $\xi = 50/311$.

necessary. We consider the spectral representation of the Euclidean two-point function

$$\begin{aligned} \langle \mathcal{O}(\bar{x}) \mathcal{O}'(0,0) \rangle &= \sum_{n=0}^{\infty} \sum_{i_1 \dots i_n} \left(\prod_{k=1}^n \int_{-\infty}^{\infty} \frac{d\theta_k}{2\pi} \right) F_{i_1 \dots i_n}^{\mathcal{O}}(\theta_1, \theta_2, \dots, \theta_n) \times \\ &\quad F_{i_1 \dots i_n}^{\mathcal{O}'}(\theta_1, \theta_2, \dots, \theta_n)^+ \exp \left(-R \sum_{k=1}^n m_{i_k} \cosh \theta_k \right) \end{aligned} \quad (4.1)$$

where

$$F_{i_1 \dots i_n}^{\mathcal{O}'}(\theta_1, \theta_2, \dots, \theta_n)^+ = {}_{i_1 \dots i_n} \langle \theta_1, \dots, \theta_n | \mathcal{O}'(0,0) | 0 \rangle = F_{i_1 \dots i_n}^{\mathcal{O}'}(\theta_1 + i\pi, \theta_2 + i\pi, \dots, \theta_n + i\pi)$$

(which is just the complex conjugate of $F_n^{\mathcal{O}'}$ for unitary theories) and $R = \sqrt{\tau^2 + x^2}$ is the length of the Euclidean separation vector $\bar{x} = (\tau, x)$.

In finite volume L , the space of states can still be labeled by multi-particle states but the momenta (and therefore the rapidities) are quantized. Denoting the quantum numbers I_1, \dots, I_n the two-point function of the same local operator can be written as

$$\begin{aligned} \langle \mathcal{O}(\tau,0) \mathcal{O}'(0,0) \rangle_L &= \sum_{n=0}^{\infty} \sum_r \sum_{I_1 \dots I_n} \langle 0 | \mathcal{O}(0,0) | \{I_1, I_2, \dots, I_n\} \rangle_L^{(r)} \times \\ &\quad {}^{(r)} \langle \{I_1, I_2, \dots, I_n\} | \mathcal{O}'(0,0) | 0 \rangle_L \exp \left(-\tau \sum_{k=1}^n m_{i_k} \cosh \theta_k \right) \end{aligned} \quad (4.2)$$

where the index r enumerates the eigenvector of the n -particle transfer matrix (as an example cf. Appendix A where these are constructed for sine-Gordon solitons); these are usually rapidity dependent linear combinations in the space of particle multiplet indices $i_1 \dots i_n$. We can assume that the wave function amplitudes (A.1) of these states are normalized and form a complete basis:

$$\begin{aligned} \sum_{i_1 \dots i_n} \Psi_{i_1 \dots i_n}^{(r)}(\{\theta_k\}) \Psi_{i_1 \dots i_n}^{(s)}(\{\theta_k\})^* &= \delta_{rs} \\ \sum_r \Psi_{i_1 \dots i_n}^{(r)}(\{\theta_k\}) \Psi_{j_1 \dots j_n}^{(r)}(\{\theta_k\})^* &= \delta_{i_1 j_1} \dots \delta_{i_n j_n} \end{aligned}$$

In writing (4.2) we also supposed that the finite volume multi-particle states $|\{I_1, I_2, \dots, I_n\}\rangle_{r,L}$ are orthonormal and for simplicity restricted the formula to separation in Euclidean time τ only. The index L signals that the matrix element is evaluated in finite volume L . Using the finite volume expansion developed by Lüscher in [43] one can easily see that

$$\langle \mathcal{O}(\tau,0) \mathcal{O}'(0) \rangle - \langle \mathcal{O}(\tau,0) \mathcal{O}'(0) \rangle_L \sim O(e^{-\mu L}) \quad (4.3)$$

where μ is some characteristic mass scale.

We can now rewrite the infinite volume correlator in the basis of multi-particle transfer matrix eigenstates

$$\begin{aligned} \langle \mathcal{O}(\tau,0) \mathcal{O}'(0,0) \rangle &= \sum_{n=0}^{\infty} \sum_r \left(\prod_{k=1}^n \int_{-\infty}^{\infty} \frac{d\theta_k}{2\pi} \right) F^{\mathcal{O}}(\theta_1, \dots, \theta_n)^{(r)} \times \\ &\quad F^{\mathcal{O}'}(\theta_1, \dots, \theta_n)^{(r)+} \exp \left(-\tau \sum m_{i_k} \cosh \theta_k \right) \end{aligned}$$

where

$$F^{\mathcal{O}}(\theta_1, \dots, \theta_n)^{(r)} = \sum_{i_1 \dots i_n} F_{i_1 \dots i_n}^{\mathcal{O}}(\theta_1, \dots, \theta_n) \Psi_{i_1 \dots i_n}^{(r)}(\{\theta_k\})$$

The remainder of the argument follows the lines of the paper [24]. Essentially, we compare the discrete sum with the integral, and realize that up to exponentially small terms in L the relation is given by the Jacobian of the mapping between the quantum number and the rapidity space, i.e. the density of states. We obtain

$$\left| \langle 0 | \mathcal{O}(0, 0) | \{I_1, \dots, I_n\} \rangle_L^{(r)} \right| = \left| \frac{F^{\mathcal{O}}(\tilde{\theta}_1, \dots, \tilde{\theta}_n)^{(r)}}{\sqrt{\rho^{(r)}(\tilde{\theta}_1, \dots, \tilde{\theta}_n)}} \right| + O(e^{-\mu' L}) \quad (4.4)$$

where³

$$\rho^{(r)}(\theta_1, \dots, \theta_n)$$

is the density of states with internal wave vector $\Psi^{(r)}$ as given in (A.4), and $\tilde{\theta}_k$ are the solutions of the Bethe-Yang equations (A.3) corresponding to the state with the specified quantum numbers I_1, \dots, I_n at the given volume L .

This can be easily generalized to matrix elements with no disconnected pieces:

$$\begin{aligned} \left| {}^{(s)} \langle \{I'_1, \dots, I'_M\} | \mathcal{O}(0, 0) | \{I_1, \dots, I_N\} \rangle_L^{(r)} \right| = \\ \left| \frac{F^{\mathcal{O}}(\tilde{\theta}'_M, \dots, \tilde{\theta}'_1 | \tilde{\theta}_1, \dots, \tilde{\theta}_N)^{(s,r)}}{\sqrt{\rho^{(r)}(\tilde{\theta}_1, \dots, \tilde{\theta}_N) \rho^{(s)}(\tilde{\theta}'_1, \dots, \tilde{\theta}'_M)}} \right| + O(e^{-\mu' L}) \end{aligned} \quad (4.5)$$

where

$$\begin{aligned} F^{\mathcal{O}}(\tilde{\theta}'_M, \dots, \tilde{\theta}'_1 | \tilde{\theta}_1, \dots, \tilde{\theta}_N)^{(s,r)} \\ = \sum_{j_1 \dots j_M} \sum_{i_1 \dots i_N} \Psi_{j_1 \dots j_M}^{(s)} \left(\left\{ \tilde{\theta}'_k \right\} \right)^* F_{j_M \dots j_1 i_1 \dots i_N}^{\mathcal{O}}(\tilde{\theta}'_M + i\pi, \dots, \tilde{\theta}'_1 + i\pi, \tilde{\theta}_1, \dots, \tilde{\theta}_N) \Psi_{i_1 \dots i_N}^{(r)} \left(\left\{ \tilde{\theta}_k \right\} \right) \end{aligned}$$

where the bar denotes the antiparticle.

This can be easily applied to soliton-antisoliton states. The algebraic Bethe Ansatz gives two eigenvectors in this subspace (cf. A.3):

$$B(\lambda_1) \Omega \propto \begin{cases} v_{+-} + v_{-+} & \text{for } \lambda_1 = \frac{\theta_1 + \theta_2}{2} + i\frac{\pi}{2} \\ v_{+-} - v_{-+} & \text{for } \lambda_1 = \frac{\theta_1 + \theta_2}{2} + i\frac{(1+\xi)\pi}{2} \end{cases}$$

i.e.

$$\begin{aligned} \Psi^{(+)} &= \frac{1}{\sqrt{2}}(0, +1, +1, 0) \\ \Psi^{(-)} &= \frac{1}{\sqrt{2}}(0, +1, -1, 0) \end{aligned}$$

Since the value of the magnonic variable λ_1 is explicitly known, it can be eliminated from the Bethe-Yang equations, resulting in the following quantization conditions for the soliton-antisoliton pair:

$$\begin{aligned} Q_1^{(\pm)}(\theta_1, \theta_2) &= ML \sinh \theta_1 - i \log \mathcal{S}_{\pm}(\theta_1 - \theta_2) = 2\pi I_1 \\ Q_2^{(\pm)}(\theta_1, \theta_2) &= ML \sinh \theta_2 - i \log \mathcal{S}_{\pm}(\theta_2 - \theta_1) = 2\pi I_2 \end{aligned} \quad (4.6)$$

³We note that μ' is not necessarily the same scale as in (4.3) and its value depends on the spectrum and bound state fusion angles of the model.

where \mathcal{S}_\pm are the eigenvalues of the two-particle S -matrix given in (A.2) and the \pm distinguishes the two states. It is also easy to eliminate the magnon λ_1 from the density of states to obtain

$$\rho^{(\pm)}(\theta_1, \theta_2) = \left| \begin{array}{cc} \frac{\partial Q_1^{(\pm)}}{\partial \theta_1} & \frac{\partial Q_1^{(\pm)}}{\partial \theta_2} \\ \frac{\partial Q_2^{(\pm)}}{\partial \theta_1} & \frac{\partial Q_2^{(\pm)}}{\partial \theta_2} \end{array} \right|$$

From (4.4) we obtain

$$\left| \langle 0 | \mathcal{O}(0, 0) | \{I_1, I_2\} \rangle_L^{(\pm)} \right| = \frac{|F^\pm(\tilde{\theta}_1 - \tilde{\theta}_2)|}{\sqrt{\rho^{(\pm)}(\tilde{\theta}_1, \tilde{\theta}_2)}} + O(e^{-\mu L}) \quad (4.7)$$

where

$$F^\pm(\theta) = \frac{1}{\sqrt{2}} \left(F_{+-}^\beta(\theta) \pm F_{-+}^\beta(\theta) \right)$$

in terms of (2.9) and $\tilde{\theta}_{1,2}$ are the solutions of (4.6) at the given volume L with quantum numbers $I_{1,2}$.

At the moment, there is no general theoretical result for matrix elements with disconnected pieces (e.g. diagonal ones). However, for one-soliton matrix elements one can easily write down the appropriate generalization of eqn. (3.4):

$$_+\langle \{I\} | \mathcal{O}(0, 0) | \{I\} \rangle_+ = \frac{F_{-+}(-i\pi)}{ML \cosh \tilde{\theta}} + \mathcal{G}_1(\beta) \quad (4.8)$$

where F_{-+} is given in (2.9) and the rapidity $\tilde{\theta}$ is quantized as

$$ML \sinh \tilde{\theta} = 2\pi I$$

4.2 Numerical verification of solitonic matrix elements

The formulae derived in the previous subsection show an excellent agreement with TCSA. Figure 4.1 demonstrates this for the matrix element between the vacuum and the (symmetric or antisymmetric) soliton-antisoliton two-particle states as given in eqn. (4.7). We can also study one-soliton-one-soliton matrix elements. For the non-diagonal ones we can use the $N = M = 1$ case of (4.5) while for the diagonal ones it turns out we must slightly modify (4.8) by changing the sign of the F_{-+} term:

$$_+\langle \{I\} | \mathcal{O}(0, 0) | \{I\} \rangle_+ = -\frac{F_{-+}(-i\pi)}{ML \cosh \tilde{\theta}} + \mathcal{G}_1(\beta) \quad (4.9)$$

It is not yet clear to us what is the reason behind this, but, as shown in figure 4.2 this produces an excellent agreement with the TCSA data. It is possible that the bootstrap solution (2.9) is off by a sign⁴, or that the sign here is related in some way to the crossing of a soliton.

5 Conclusions and outlook

In this work we investigated the comparison between form factors of sine-Gordon theory obtained from the bootstrap and finite volume matrix elements given by the truncated

⁴This would not be detected by checking off-diagonal matrix elements, since due to phase differences these compare only the absolute values according to (4.5).

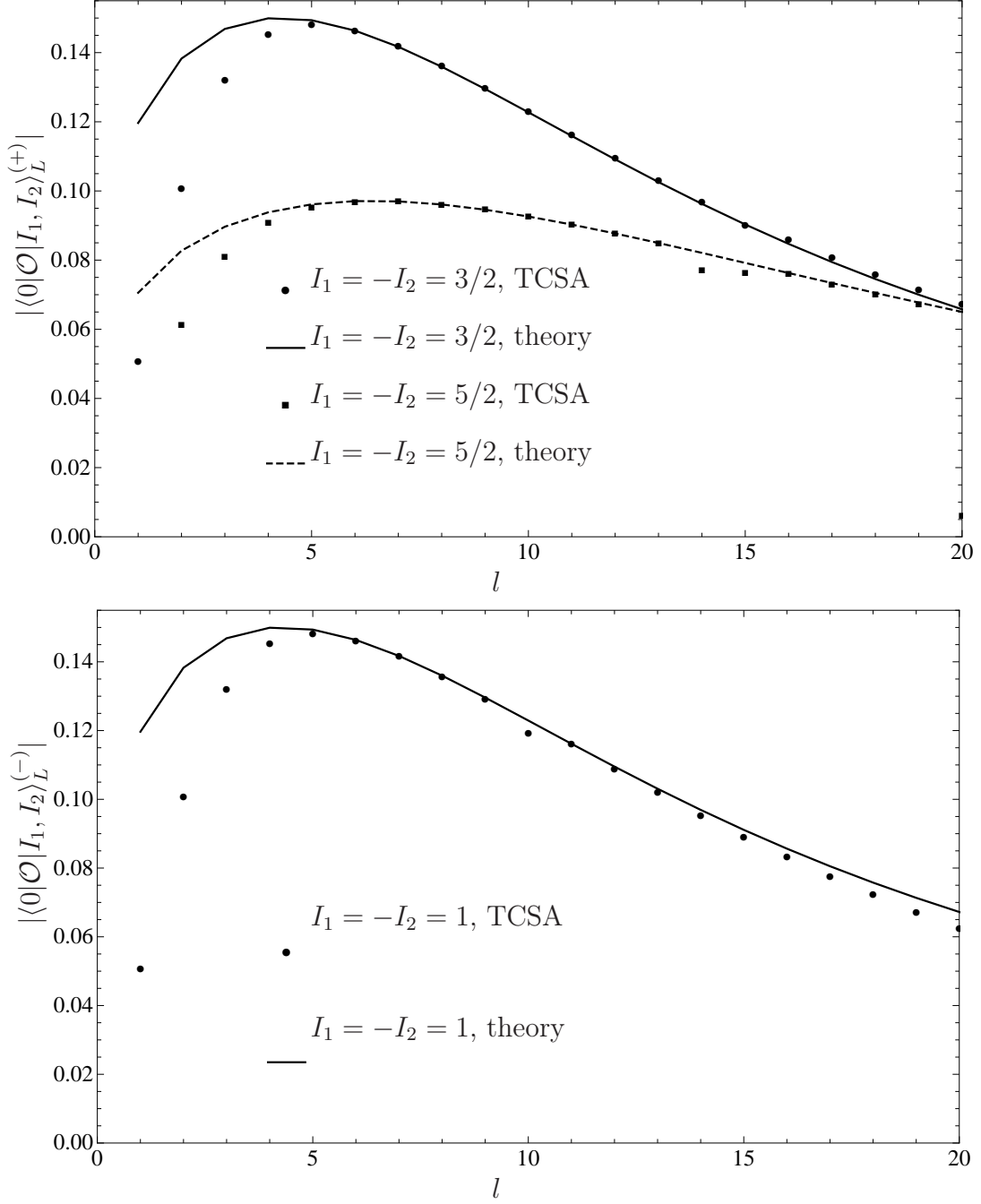


Figure 4.1: Vacuum-soliton-antisoliton form factors at $\xi = 2/7$. The individual deviations are caused by the proximity of level crossings.

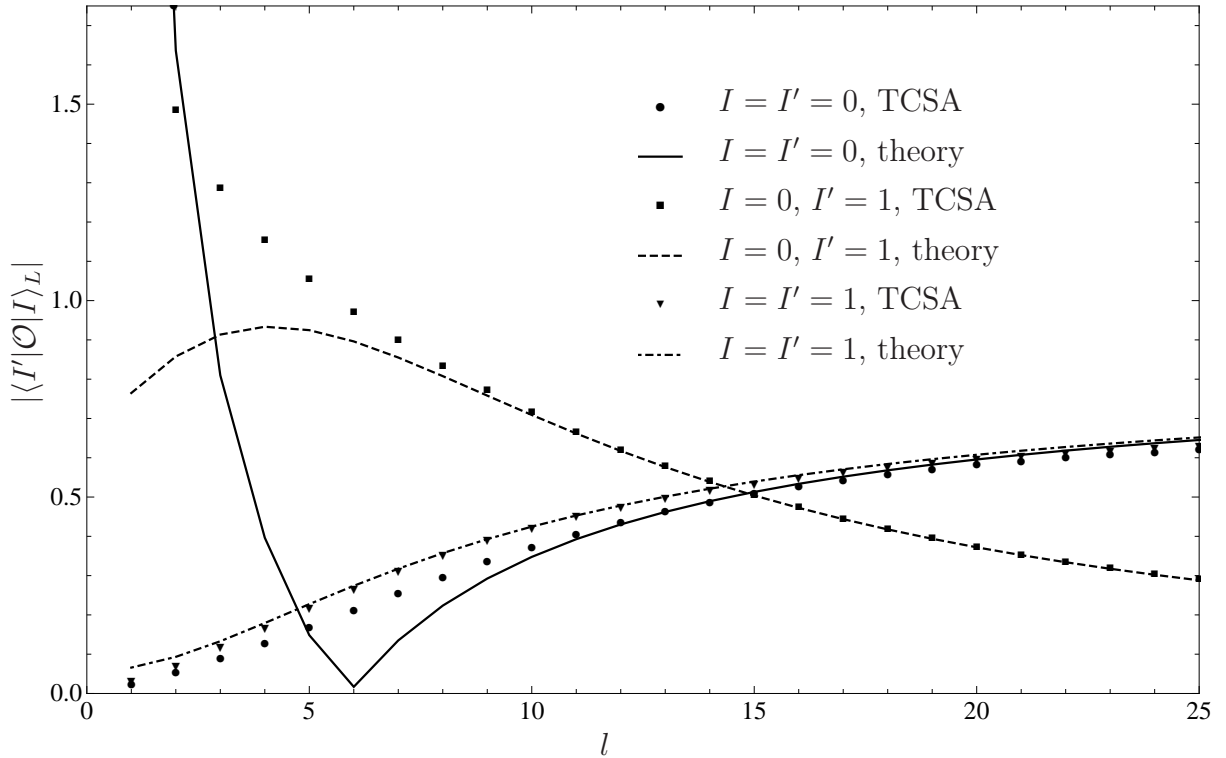


Figure 4.2: Soliton–soliton form factors: off-diagonal and diagonal case at $\xi = 50/239$. The cusp in the continuous line is an artifact caused by taking the absolute value.

conformal space approach. Generally speaking, we found an excellent agreement between the theoretical predictions and the numerical results. We also generalized the formalism developed in [24, 25] to non-diagonal scattering theory in order to include solitonic matrix elements in the test.

In this latter respect, however, several problems are still open. One of them is to find a suitable formula for matrix elements with disconnected contributions in the case of non-diagonal scattering (at present we only have the simplest, one-particle–one-particle case covered). The other, more technical problem is to find a suitable framework for the numerical evaluation of the multi-soliton form factors; until then, the full strength of the algebraic Bethe Ansatz formalism presented in Appendix A cannot be utilized. In addition, the solution of the problem in the case of diagonal $B_1 B_1 - B_1 B_1$ matrix elements, described in subsection 3.4, also hinges on the ability of handling such matrix elements. A further issue is the presence of the minus sign in (4.9) which requires a detailed look into the soliton form factor bootstrap, which is out of the scope of present work.

Another interesting issue is the role played by the so-called μ -terms, which are exponential corrections to the volume dependence of the matrix elements resulting from particle fusions (in other words, three-particle couplings between on-shell particle states). The exponential decay of these corrections depends only on the mass spectrum; however, their strength is also determined by appropriate form factors, as illustrated in subsection 3.3 by the fact that for the same B_2 state (hence the same μ -term kinematics), the significance of the corrections depends very much on the matrix element the state is involved in.

In this work we generally took the stance of using the bootstrap results to predict the numerical finite volume results. However, one could take the opposite route and extract field theoretically interesting matrix elements from the finite volume data (which we also did for cases involving two-particle matrix elements). This is common in lattice field theory and was advocated by Lellouch and Lüscher in [44] as a way to circumvent the so-called

Maiani-Testa no-go theorem [45]. We have previously used a similar approach to determine resonance parameters from finite volume spectra [46].

The μ -term results have an implication for such studies, which aim to determine matrix elements (e.g. related to weak interaction) from finite volume data (whether using lattice Monte-Carlo or some other numerical method). The important lesson is that even if the appropriate exponential factor μ (as determined by the mass spectrum) is not small and therefore volume suppression is expected to be strong, the μ -term can still have a sizable effect at the values of volume the applied numerical method (whether TCSA or lattice) can reach. In addition, this term could vary strongly between different matrix elements involving the same state, thereby producing very large systematic errors when extracting matrix elements of local operators from numerical simulations (indeed, the corrections could be of the order of 100% as illustrated by the $B_2 - B_1$ matrix element plotted in figure 3.7).

Acknowledgments

GT is grateful to B. Pozsgay for useful discussions. This work was partially supported by the Hungarian OTKA grants K75172 and K81461.

A Algebraic Bethe Ansatz for multi-soliton states

A.1 The sine-Gordon soliton Bethe-Yang equations and the multi-particle transfer matrix

Our starting object is the N -particle monodromy matrix that can be written as

$$\mathcal{M}(\lambda | \{\theta_1, \dots, \theta_N\})_{a, i_1 \dots i_N}^{b, j_1 \dots j_N} = \mathcal{S}_{a i_1}^{c_1 j_1}(\lambda - \theta_1) \mathcal{S}_{c_1 i_2}^{c_2 j_2}(\lambda - \theta_2) \dots \mathcal{S}_{c_{N-1} i_N}^{b j_N}(\lambda - \theta_N)$$

or as a 2×2 matrix in the a, b indices

$$\mathcal{M}(\lambda | \{\theta_k\}) = \begin{pmatrix} A(\lambda | \{\theta_k\}) & B(\lambda | \{\theta_k\}) \\ C(\lambda | \{\theta_k\}) & D(\lambda | \{\theta_k\}) \end{pmatrix}$$

The operators A, B, C and D act in the 2^N -dimensional “isospin” space (the space spanned by the N soliton doublets)

$$\mathcal{V}_N = \bigotimes_{k=1}^n \mathbb{C}^2$$

which is spanned by the basis

$$v_{i_1 \dots i_N} \quad , \quad i_k = \pm$$

One can introduce the vector

$$\Omega = v_{++++}$$

corresponding to all solitons being positively charged. The general transfer matrix

$$\mathcal{T}(\lambda | \{\theta_k\}) = \mathcal{M}(\lambda | \{\theta_k\})_a^a = A(\lambda | \{\theta_k\}) + D(\lambda | \{\theta_k\})$$

gives rise to the specified transfer matrices

$$\tau_j(\{\theta_k\}) = \mathcal{T}(\lambda = \theta_j | \{\theta_k\})$$

In terms of these the n -particle quantization relations, ie. the Bethe-Yang equations on the circle can be written as [47]

$$e^{iML \sinh \theta_j} \tau_j(\{\theta_k\}) \Psi(\{\theta_k\}) = \Psi(\{\theta_k\})$$

where $\Psi(\{\theta_k\}) \in \mathcal{V}_N$ is the wave-function amplitude vector.

A.2 The Algebraic Bethe Ansatz

We use the well-established machinery of the algebraic Bethe Ansatz (for a pedagogical introduction see [48]). The sine-Gordon S -matrix satisfies the Yang-Baxter equations

$$\mathcal{S}_{k_2 k_3}^{j_2 j_3}(\theta_{23}) \mathcal{S}_{k_1 i_3}^{j_1 k_3}(\theta_{13}) \mathcal{S}_{i_1 i_2}^{k_1 k_2}(\theta_{12}) = \mathcal{S}_{k_1 k_2}^{j_1 j_2}(\theta_{12}) \mathcal{S}_{i_1 k_3}^{k_1 j_3}(\theta_{13}) \mathcal{S}_{i_2 i_3}^{k_2 k_3}(\theta_{23})$$

where $\theta_{ij} = \theta_i - \theta_j$. As a result, the monodromy matrix satisfies the relations

$$\mathcal{S}_{b_1 b_2}^{c_1 c_2}(\lambda - \mu) \mathcal{M}(\lambda | \{\theta_k\})_{a_1}^{b_1} \mathcal{M}(\mu | \{\theta_k\})_{a_2}^{b_2} = \mathcal{M}(\mu | \{\theta_k\})_{d_1}^{c_1} \mathcal{M}(\lambda | \{\theta_k\})_{d_2}^{c_2} \mathcal{S}_{c_1 c_2}^{d_1 d_2}(\lambda - \mu)$$

Therefore the transfer matrices form a commuting family

$$\mathcal{T}(\lambda | \{\theta_k\}) \mathcal{T}(\mu | \{\theta_k\}) = \mathcal{T}(\mu | \{\theta_k\}) \mathcal{T}(\lambda | \{\theta_k\})$$

and can be diagonalized simultaneously with common eigenvectors for all λ :

$$\mathcal{T}(\lambda | \{\theta_k\}) \psi_\alpha(\{\theta_k\}) = \Lambda_\alpha(\lambda | \{\theta_k\}) \psi_\alpha(\{\theta_k\})$$

where $\Lambda_\alpha(\lambda | \{\theta_k\}) \in S^1$ are the eigenvalues, $\psi_\alpha(\{\theta_k\}) \in \mathcal{V}_n$ are the eigenvectors and $\alpha = 1 \dots 2^N$. The independent solutions of the Bethe equations for the wave vector are then given by

$$\Psi(\{\theta_k\}) = \psi_\alpha(\{\theta_k\})$$

provided the particle rapidities satisfy the Bethe-Yang equations

$$e^{iML \sinh \theta_j} \Lambda_\alpha(\theta_j | \{\theta_k\}) = 1 \quad j = 1 \dots N$$

In this way we reduced the problem to finding the eigenvalues of the transfer matrix and then solving a system of N coupled scalar equations.

Note that the sine-Gordon scattering preserves the solitonic charge \mathcal{Q} and charge parity \mathcal{C} , which act on \mathcal{V}_N as follows:

$$\begin{aligned} \mathcal{Q} v_{i_1 \dots i_N} &= \left(\sum_{k=1}^N i_k \right) v_{i_1 \dots i_N} \\ \mathcal{C} v_{i_1 \dots i_N} &= v_{\bar{i}_1 \dots \bar{i}_N} \quad \text{where } \bar{i} = -i \end{aligned}$$

The transfer matrix \mathcal{T} commutes with these operators. In addition, B and C act as lowering and raising operators in charge space

$$\begin{aligned} [\mathcal{Q}, B(\lambda | \{\theta_k\})] &= -2B(\lambda | \{\theta_k\}) \\ [\mathcal{Q}, C(\lambda | \{\theta_k\})] &= +2C(\lambda | \{\theta_k\}) \end{aligned}$$

We now look for the eigenvectors of the transfer matrix in the form

$$\Psi(\{\lambda_s\} | \{\theta_k\}) = \mathcal{N}_\Psi B(\lambda_1 | \{\theta_k\}) \dots B(\lambda_r | \{\theta_k\}) \Omega \quad (\text{A.1})$$

where λ_s are the so-called 'magnons' and \mathcal{N}_Ψ is some normalization factor. They satisfy the eigenvalue equations

$$\mathcal{T}(\lambda | \{\theta_1, \dots, \theta_n\}) \Psi(\{\lambda_s\} | \{\theta_k\}) = \Lambda(\lambda, \{\lambda_s\} | \{\theta_k\}) \Psi(\{\lambda_s\} | \{\theta_k\})$$

provided the algebraic Bethe Ansatz (ABA) equations hold

$$\prod_{k=1}^N a(\lambda_j - \theta_k) = \prod_{k \neq j}^r \frac{a(\lambda_j - \lambda_k)}{a(\lambda_k - \lambda_j)} \quad a(\theta) = \frac{1}{S_T(\theta, \xi)} = \frac{\sinh\left(\frac{i\pi - \theta}{\xi}\right)}{\sinh\left(\frac{\theta}{\xi}\right)}$$

The eigenvalue is given by

$$\begin{aligned} \Lambda(\lambda, \{\lambda_s\} | \{\theta_1, \dots, \theta_N\}) &= \left(\prod_{k=1}^r S_T(\lambda_k - \lambda)^{-1} + \prod_{k=1}^N S_T(\lambda - \theta_k, \xi) \prod_{k=1}^r S_T(\lambda - \lambda_k)^{-1} \right) \\ &\times \prod_{k=1}^N S_0(\lambda - \theta_k, \xi) \end{aligned}$$

Notice that $a(\theta)$ (and therefore the ABA equations) has the natural periodicity

$$a(\theta + i\pi\xi) = a(\theta)$$

A.3 The two-particle case ($N = 2$)

The only interesting eigenvectors are the ones in the $\mathcal{Q} = 0$ subspace, for which we can write the Ansatz

$$B(\lambda_1)\Omega$$

The single ABA equation takes the form

$$a(\lambda_1 - \theta_1)a(\lambda_1 - \theta_2) = \frac{\sinh\left(\frac{i\pi - \lambda_1 + \theta_1}{\xi}\right) \sinh\left(\frac{i\pi - \lambda_1 + \theta_2}{\xi}\right)}{\sinh\left(\frac{\lambda_1 - \theta_1}{\xi}\right) \sinh\left(\frac{\lambda_1 - \theta_2}{\xi}\right)} = 1$$

and (up to periodicity) has two independent solutions

$$\begin{aligned} (1) \quad &: \quad \lambda_1 = \frac{\theta_1 + \theta_2}{2} + i\frac{\pi}{2} \\ (2) \quad &: \quad \lambda_1 = \frac{\theta_1 + \theta_2}{2} + i\pi\frac{1 + \xi}{2} \end{aligned}$$

We can then evaluate the corresponding eigenvalues:

$$\Lambda(\lambda, \{\lambda_1\} | \{\theta_1, \theta_2\}) = \left(\frac{1}{S_T(\lambda_1 - \lambda)} + \frac{S_T(\lambda - \theta_1)S_T(\lambda - \theta_2)}{S_T(\lambda - \lambda_1)} \right) S_0(\lambda - \theta_1)S_0(\lambda - \theta_2)$$

Putting $\lambda = \theta_1$ (to get the Bethe-Yang phase-shift for the first particle) we find

$$\begin{aligned} (1) \quad &: \quad \Lambda(\theta_1, \{\lambda_1\} | \{\theta_1, \theta_2\}) = -\mathcal{S}_+(\theta_1 - \theta_2) \\ (2) \quad &: \quad \Lambda(\theta_1, \{\lambda_1\} | \{\theta_1, \theta_2\}) = -\mathcal{S}_-(\theta_1 - \theta_2) \end{aligned}$$

where

$$\mathcal{S}_{\pm}(\theta) = (S_T(\theta) \pm S_R(\theta)) S_0(\theta) \tag{A.2}$$

are the eigenvalues of the two-particle S matrix in the neutral subspace.

A.4 The four-particle case ($N = 4$)

Albeit we are not able to use them for detailed numerical comparison yet, we briefly review the four-particle results to give a better understanding of what follows. Suppose that the four rapidities are ordered as

$$\theta_1 < \theta_2 < \theta_3 < \theta_4$$

A.4.1 $Q = 2$ sector

This subspace is four dimensional, and with the Ansatz

$$B(\lambda_1)\Omega$$

there are two types of solutions:

- $\lambda_1 = \mu + i\frac{\pi}{2}$
There are three such solutions, typically one with μ the between θ_2 and θ_3 , one around θ_1 and another one around θ_4 .
- $\lambda_1 = \mu + i(1 + \xi)\frac{\pi}{2}$
There is a single solution, with μ the between θ_2 and θ_3 .

A.4.2 $Q = 0$ sector

There are 6 eigenvectors here, which can be classified by their parity under charge conjugation \mathcal{C} . The Ansatz is

$$B(\lambda_1)B(\lambda_2)\Omega$$

and the ABA equations are

$$\prod_{k=1}^4 S_T(\lambda_1 - \theta_k) = \frac{S_T(\lambda_1 - \lambda_2)}{S_T(\lambda_2 - \lambda_1)} \quad \prod_{k=1}^4 S_T(\lambda_2 - \theta_k) = \frac{S_T(\lambda_2 - \lambda_1)}{S_T(\lambda_1 - \lambda_2)}$$

For the three $\mathcal{C} = -1$ eigenvectors, the magnons take the form

$$\lambda_1 = \mu_1 + \frac{i\pi}{2} \quad \lambda_2 = \mu_2 + \frac{i(1 + \xi)\pi}{2}$$

with the positions

$$\begin{aligned} & \theta_1 < \mu_1 < \theta_2 < \theta_3 < \mu_2 < \theta_4 \\ \text{or} \quad & \theta_1 < \mu_2 < \theta_2 < \theta_3 < \mu_1 < \theta_4 \\ \text{or} \quad & \theta_1 < \theta_2 < \mu_1, \mu_2 < \theta_3 < \theta_4 \end{aligned}$$

There are three $\mathcal{C} = +1$ eigenvectors. One has magnons of the form

$$\lambda_1 = \mu_1 + \frac{i\pi}{2} \quad \lambda_2 = \mu_2 + \frac{i\pi}{2}$$

and another one with

$$\lambda_1 = \mu_1 + \frac{i(1 + \xi)\pi}{2} \quad \lambda_2 = \mu_2 + \frac{i(1 + \xi)\pi}{2}$$

with the typical positions

$$\theta_1 < \mu_1 < \theta_2 < \theta_3 < \mu_2 < \theta_4$$

The last eigenvector is of the type

$$\lambda_1 = \mu + \frac{i\pi(1 + x)}{2} \quad \lambda_2 = \mu + \frac{i\pi(1 - x)}{2}$$

where μ is exactly

$$\mu = \frac{\theta_1 + \theta_2 + \theta_3 + \theta_4}{4}$$

and the fundamental range of x is

$$0 < x < \xi/2$$

given that the algebraic Bethe Ansatz has periodicity $i\pi\xi$ (and the sign of x does not matter).

A.5 The density of states

The quantization conditions for the multi-soliton states can be written as follows:

$$\begin{aligned} e^{iML \sinh \theta_j} \Lambda(\theta_j, \{\lambda_1, \dots, \lambda_r\} | \{\theta_1, \dots, \theta_N\}) &= 1, \quad j = 1, \dots, N \\ \prod_{k=1}^N a(\lambda_j - \theta_k) \prod_{k \neq j}^r \frac{a(\lambda_k - \lambda_j)}{a(\lambda_j - \lambda_k)} &= 1, \quad j = 1, \dots, r \end{aligned} \quad (\text{A.3})$$

where N is the number of solitonic particles and $\mathcal{Q} = N - 2r$ is their total topological charge. The magnonic configuration as detailed in the previous subsection fixes the “isospin” structure of the state in the 2^N dimensional internal charge space. The two equations must be solved simultaneously. In principle, the positions of the magnons are fixed in terms of the rapidities $\theta_1, \dots, \theta_N$ so the density of states with a given N , r and fixed isospin structure can be computed from the quantization relations of the solitons

$$Q_j(\theta_1, \dots, \theta_N | \lambda_1, \dots, \lambda_r) = ML \sinh \theta_j - i \log \Lambda(\theta_j, \{\lambda_1, \dots, \lambda_r\} | \{\theta_1, \dots, \theta_N\}) = 2\pi I_j$$

by taking the Jacobi determinant of the rapidity \mapsto quantum numbers mapping [24]

$$\rho(\theta_1, \dots, \theta_N) = \det \left(\frac{\partial Q_j}{\partial \theta_k} \right)_{j,k=1, \dots, N}$$

where it is understood that we differentiate also the dependence of the λ_s with respect to the rapidities. However, there is an easier way to obtain the density of states by extending the set of BY equations by those of the magnons, considering also the magnonic quantization relations

$$\mathcal{M}_j(\theta_1, \dots, \theta_N | \lambda_1, \dots, \lambda_r) = -i \sum_{k=1}^N \log a(\lambda_j - \theta_k) - i \sum_{k \neq j}^r \log \frac{a(\lambda_k - \lambda_j)}{a(\lambda_j - \lambda_k)} = 0$$

Then one has the following result

$$\rho(\theta_1, \dots, \theta_N) = \left(\det \frac{\partial(Q, \mathcal{M})}{\partial(\theta, \lambda)} / \det \frac{\partial \mathcal{M}}{\partial \lambda} \right) \Big|_{\lambda_s \rightarrow \lambda_s(\theta_1, \dots, \theta_N)} \quad (\text{A.4})$$

where the first determinant is the $(N+r) \times (N+r)$ Jacobi determinant formed by including the magnonic equations, differentiating by keeping the θ_k and λ_j independent, and the second is the $r \times r$ one containing only the magnonic relations. This can be proven with a bit of labour by expressing the derivatives

$$\frac{\partial \lambda_j}{\partial \theta_k}$$

by differentiating the magnonic relations and using simple properties of determinants. However, the result is very easy to understand intuitively. Since the magnons do not have independently chosen quantum numbers (their position is fixed by the rapidities of the solitons), the solitonic phase space volume can be obtained from the phase space volume calculated with all variables (rapidities and magnons) involved, divided by the volume contribution of the magnons themselves.

References

- [1] A. B. Zamolodchikov and A. B. Zamolodchikov, “Factorized S-matrices in two dimensions as the exact solutions of certain relativistic quantum field models,” *Annals Phys.* **120** (1979) 253–291.
- [2] G. Mussardo, “Off critical statistical models: Factorized scattering theories and bootstrap program,” *Phys. Rept.* **218** (1992) 215–379.
- [3] M. Karowski and P. Weisz, “Exact Form-Factors in (1+1)-Dimensional Field Theoretic Models with Soliton Behavior,” *Nucl. Phys.* **B139** (1978) 455.
- [4] A. N. Kirillov and F. A. Smirnov, “A representation of the current algebra connected with the SU(2) invariant Thirring model,” *Phys. Lett.* **B198** (1987) 506–510.
- [5] F. A. Smirnov, “Form-factors in completely integrable models of quantum field theory,” *Adv. Ser. Math. Phys.* **14** (1992) 1–208.
- [6] Z. Bajnok, L. Palla, and G. Takacs, “On the boundary form factor program,” *Nucl. Phys.* **B750** (2006) 179–212, [arXiv:hep-th/0603171](#).
- [7] G. Takacs, “Form factors of boundary exponential operators in the sinh-Gordon model,” *Nucl. Phys.* **B801** (2008) 187–206, [arXiv:0801.0962](#).
- [8] A. Koubek and G. Mussardo, “On the operator content of the sinh-Gordon model,” *Phys. Lett.* **B311** (1993) 193–201, [arXiv:hep-th/9306044](#).
- [9] A. Koubek, “A Method to determine the operator content of perturbed conformal field theories,” *Phys. Lett.* **B346** (1995) 275–283, [arXiv:hep-th/9501028](#).
- [10] A. Koubek, “Form-factor bootstrap and the operator content of perturbed minimal models,” *Nucl. Phys.* **B428** (1994) 655–680, [arXiv:hep-th/9405014](#).
- [11] A. Koubek, “The Space of local operators in perturbed conformal field theories,” *Nucl. Phys.* **B435** (1995) 703–734, [arXiv:hep-th/9501029](#).
- [12] F. A. Smirnov, “Counting the local fields in SG theory,” *Nucl. Phys.* **B453** (1995) 807–824, [arXiv:hep-th/9501059](#).
- [13] V. P. Yurov and A. B. Zamolodchikov, “Correlation functions of integrable 2-D models of relativistic field theory. Ising model,” *Int. J. Mod. Phys.* **A6** (1991) 3419–3440.
- [14] A. B. Zamolodchikov, “Two point correlation function in scaling Lee-Yang model,” *Nucl. Phys.* **B348** (1991) 619–641.
- [15] A. B. Zamolodchikov, “Irreversibility of the Flux of the Renormalization Group in a 2D Field Theory,” *JETP Lett.* **43** (1986) 730–732.
- [16] J. L. Cardy, “The central charge and universal combinations of amplitudes in two-dimensional theories away from criticality,” *Phys. Rev. Lett.* **60** (1988) 2709.
- [17] A. Cappelli, D. Friedan, and J. I. Latorre, “C theorem and spectral representation,” *Nucl. Phys.* **B352** (1991) 616–670.

- [18] D. Z. Freedman, J. I. Latorre, and X. Vilasis, “Illustrating the spectral form of the C theorem,” *Mod. Phys. Lett. A* **6** (1991) 531–542.
- [19] G. Delfino, P. Simonetti, and J. L. Cardy, “Asymptotic factorisation of form factors in two- dimensional quantum field theory,” *Phys. Lett. B* **387** (1996) 327–333, [arXiv:hep-th/9607046](#).
- [20] F. A. Smirnov, “Quasi-classical study of form factors in finite volume,” [arXiv:hep-th/9802132](#).
- [21] V. E. Korepin and N. A. Slavnov, “Form Factors in the Finite Volume,” *International Journal of Modern Physics B* **13** (1999) 2933–2941, [arXiv:math-ph/9812026](#).
- [22] G. Mussardo, V. Riva, and G. Sotkov, “Finite-volume form factors in semiclassical approximation,” *Nucl. Phys. B* **670** (2003) 464–478, [arXiv:hep-th/0307125](#).
- [23] B. Doyon, “Finite-temperature form factors: A review,” *SIGMA* **3** (2007) 011, [arXiv:hep-th/0611066](#).
- [24] B. Pozsgay and G. Takacs, “Form factors in finite volume I: form factor bootstrap and truncated conformal space,” *Nucl. Phys. B* **788** (2008) 167–208, [arXiv:0706.1445](#).
- [25] B. Pozsgay and G. Takacs, “Form factors in finite volume II: disconnected terms and finite temperature correlators,” *Nucl. Phys. B* **788** (2008) 209–251, [arXiv:0706.3605](#).
- [26] B. Pozsgay, “Finite volume form factors and correlation functions at finite temperature,” [arXiv:0907.4306 \[hep-th\]](#).
- [27] M. Kormos and G. Takacs, “Boundary form factors in finite volume,” *Nucl. Phys. B* **803** (2008) 277–298, [arXiv:0712.1886](#).
- [28] F. H. L. Essler and R. M. Konik, “Applications of massive integrable quantum field theories to problems in condensed matter physics,” [arXiv:cond-mat/0412421](#).
- [29] F. H. L. Essler and R. M. Konik, “Finite-temperature dynamical correlations in massive integrable quantum field theories,” *J. Stat. Mech.* **0909** (2009) P09018, [arXiv:0907.0779 \[cond-mat.str-el\]](#).
- [30] F. H. L. Essler and R. M. Konik, “Finite-temperature lineshapes in gapped quantum spin chains,” *Phys. Rev. B* **78** (2008) 100403, [arXiv:0711.2524 \[cond-mat.str-el\]](#).
- [31] G. Feverati, F. Ravanini, and G. Takacs, “Truncated conformal space at $c = 1$, nonlinear integral equation and quantization rules for multi-soliton states,” *Phys. Lett. B* **430** (1998) 264–273, [arXiv:hep-th/9803104](#).
- [32] S. L. Lukyanov and A. B. Zamolodchikov, “Exact expectation values of local fields in quantum sine-Gordon model,” *Nucl. Phys. B* **493** (1997) 571–587, [arXiv:hep-th/9611238](#).
- [33] A. B. Zamolodchikov, “Mass scale in the sine-Gordon model and its reductions,” *Int. J. Mod. Phys. A* **10** (1995) 1125–1150.

- [34] S. L. Lukyanov, “Form factors of exponential fields in the sine-Gordon model,” *Mod. Phys. Lett.* **A12** (1997) 2543–2550, [arXiv:hep-th/9703190](#).
- [35] G. Takacs, “Form factor perturbation theory from finite volume,” *Nucl. Phys.* **B825** (2010) 466–481, [arXiv:0907.2109](#).
- [36] F. A. Smirnov, “Form-factors in completely integrable models of quantum field theory,” *Adv. Ser. Math. Phys.* **14** (1992) 1–208.
- [37] S. L. Lukyanov, “Free field representation for massive integrable models,” *Commun. Math. Phys.* **167** (1995) 183–226, [arXiv:hep-th/9307196](#).
- [38] H. M. Babujian, A. Fring, M. Karowski, and A. Zapletal, “Exact form factors in integrable quantum field theories: The sine-Gordon model,” *Nucl. Phys.* **B538** (1999) 535–586, [arXiv:hep-th/9805185](#).
- [39] H. Babujian and M. Karowski, “Exact form factors in integrable quantum field theories: The sine-Gordon model. II,” *Nucl. Phys.* **B620** (2002) 407–455, [arXiv:hep-th/0105178](#).
- [40] V. P. Yurov and A. B. Zamolodchikov, “Truncated conformal space approach to scaling Lee-Yang model,” *Int. J. Mod. Phys.* **A5** (1990) 3221–3246.
- [41] Z. Bajnok, L. Palla, G. Takacs, and F. Wagner, “The k-folded sine-Gordon model in finite volume,” *Nucl. Phys.* **B587** (2000) 585–618, [arXiv:hep-th/0004181](#).
- [42] B. Pozsgay, “Luscher’s mu-term and finite volume bootstrap principle for scattering states and form factors,” *Nucl. Phys.* **B802** (2008) 435–457, [arXiv:0803.4445 \[hep-th\]](#).
- [43] M. Luscher, “Volume Dependence of the Energy Spectrum in Massive Quantum Field Theories. 1. Stable Particle States,” *Commun. Math. Phys.* **104** (1986) 177.
- [44] L. Lellouch and M. Luscher, “Weak transition matrix elements from finite-volume correlation functions,” *Commun. Math. Phys.* **219** (2001) 31–44, [arXiv:hep-lat/0003023](#).
- [45] L. Maiani and M. Testa, “Final state interactions from Euclidean correlation functions,” *Phys. Lett.* **B245** (1990) 585–590.
- [46] B. Pozsgay and G. Takacs, “Characterization of resonances using finite size effects,” *Nucl. Phys.* **B748** (2006) 485–523, [arXiv:hep-th/0604022](#).
- [47] G. Takacs and G. Watts, “Non-unitarity in quantum affine Toda theory and perturbed conformal field theory,” *Nucl. Phys.* **B547** (1999) 538–568, [arXiv:hep-th/9810006](#).
- [48] L. D. Faddeev, “How Algebraic Bethe Ansatz works for integrable model,” [arXiv:hep-th/9605187](#).